Movement of Proteins in an Environment Crowded by Surfactant Micelles: Anomalous versus Normal Diffusion

Jędrzej Szymański,[†] Adam Patkowski,[‡] Jacek Gapiński,[‡] Agnieszka Wilk,[‡] and Robert Hołyst*[,†]

Institute of Physical Chemistry, Polish Academy of Sciences, Department III, Kasprzaka 44/52, 01-224 Warsaw, Poland, and Institute of Physics, A. Mickiewicz University, Umultowska 85, 61-614 Poznań, Poland

Received: October 3, 2005; In Final Form: February 3, 2006

Small proteins move in crowded cell compartments by anomalous diffusion. In many of them, e.g., the endoplasmic reticulum, the proteins move between lipid membranes in the aqueous lumen. Molecular crowding in vitro offers a systematic way to study anomalous and normal diffusion in a well controlled environment not accessible in vivo. We prepared a crowded environment in vitro consisting of hexaethylene glycol monododecyl ether ($C_{12}E_6$) nonionic surfactant and water and observed lysozyme diffusion between elongated micelles. We have fitted the data obtained in fluorescence correlation spectroscopy using an anomalous diffusion model and a two-component normal diffusion model. For a small concentration of surfactant (below 4 wt %) the data can be fitted by single-component normal diffusion. For larger concentrations the normal diffusion fit gave two components: one very slow and one fast. The amplitude of the slow component grows with $C_{12}E_6$ concentration. The ratio of diffusion coefficients (slow to fast) is on the order of 0.1 for all concentrations of surfactant in the solution. The fast diffusion is due to free proteins while the slow one is due to the protein−micelle complexes. The protein−micelle interaction is weak since even in a highly concentrated solution (35% of $C_{12}E_6$) the amplitude of the slow mode is only 10%, despite the fact that the average distance between the micelles is the same as the size of the protein. The anomalous diffusion model gave the anomality index ($\langle r^2(t)\rangle \sim t^\alpha$), α monotonically decreasing from $\alpha = 1$ (at 4% surfactant) to $\alpha = 0.88$ (at 37% surfactant). The fits for two-component normal diffusion and anomalous diffusion were of equally good quality, but the physical interpretation was only straightforward for the former.

Introduction

In physiological compartments macromolecules and lipids form a crowded environment with concentrations up to several hundred grams per liter, occupying up to 40% of available volume.[1,2] The system is termed crowded rather than concentrated since most of the species are not present in high concentrations.[2] One of the simplest yet important problems concerning macromolecules in the crowded environment is their mobility and movement. In general the movement of proteins, which is largely determined by the distribution of matter in cell compartments, is required for numerous cellular processes including metabolism, second messenger signaling, and protein−protein interactions. Protein diffusion has been observed in various cell compartments: cytoplasm,[3,4,5] endoplasmic reticulum,[6] cell nucleus,[7] and mitochondria.[8] Most of the proteins of low molecular weight move relatively freely by diffusion in cell compartments such as the cell nucleus[7] or endoplasmic reticulum. Diffusion in the cytoplasm for the small fluorescent probe 2′,7′-bis(2-carboxyethyl)-5(6)-carboxyfluorescein (BCECF) was found to be only 4 times slower than that in water. Three mechanisms leading to the slowed diffusion were identified: higher viscosity,[9] binding, and collisions with obstacles.[10] The typical diffusion coefficients for green fluorescent protein (GFP), determined by the fluorescence recovery after photobleaching (FRAP) techniques, are as follows: in water 87 $\mu m^2/s$, in bacterial cytoplasm 7.7 $\mu m^2/s$,[4] in eukaryotic cytoplasm 27 $\mu m^2/s$ [5], mitochondria 20−30 $\mu m^2/s$,[8] and in endoplasmic reticulum 10 $\mu m^2/s$.[6,11] The latter values are not much different from the diffusion of GFP in a nucleus.[7,12]

Recent FRAP[13] experiments have shown that this technique could be successfully applied to systems exhibiting anisotropic and anomalous diffusion, although earlier[14−17] experiments reported difficulty in distinguishing between normal and anomalous diffusion, especially if we have a mobile and immobile fraction of proteins. In normal diffusion the mean-square displacement, $\langle r^2(t)\rangle$, of proteins as a function of time, t, is $\langle r^2(t)\rangle \sim t$ while anomalous diffusion leads to $\langle r^2(t)\rangle \sim t^\alpha$, where $\alpha < 1$. Moreover, all recent experimental studies using fluorescence correlation spectroscopy (FCS)[18−21] indicate that the proteins, colloids, macromolecules, and even small solute molecules move by anomalous diffusion in crowded environments in vivo or in vitro.[3,22−26] The obstacles can slow diffusion[27] and lead to anomalous diffusion on time scales depending on the concentration of obstacles. At the percolation threshold the obstacles enforce anomalous diffusion at all time and length scales. Also the fractal environment leads to anomalous diffusion on time and length scales where fractal structure shows up. Finally, diffusion in the system of traps with algebraic distribution of the escape time can also be described by anomalous diffusion.[28] Irrespective of the precise mechanism of anomalous diffusion, the cell compartments seem to have the structure and elastic properties promoting anomalous over normal diffusion. The precise determination and elucidation of the protein movement is extremely important for understanding

* Author to whom correspondence should be addressed. E-mail: holyst@ptys.ichf.edu.pl.
[†] Polish Academy of Sciences.
[‡] A. Mickiewicz University.

10.1021/jp055626w CCC: $33.50
Published on Web 03/09/2006

various processes taking place in living cells. It was recognized many years ago that free diffusion in space is too slow for many biological processes such as gene expression, gene silencing, etc. Simple estimates show that TATA binding protein needs 10^5 seconds to reach the specific site (TATA) inside a nucleus by free diffusion.[29,30] Various mechanisms have been proposed to speed up the search process for the diffusion-limited reactions: reduction of dimensionality, sliding with intersegment transfer, and a combination of three- and one-dimensional diffusion.[31,30] Nevertheless this problem is still unresolved, because we do not even know how various macromolecules in the crowded compartment are arranged in space. From this observation follows a clear need to study diffusion in crowded yet precisely known environments. In particular it is desirable to know the precise distribution of obstacles in the volume. In this way we can observe protein movement in a well controlled environment. This paper is devoted to the study of protein diffusion in surfactant solutions. Since in many biological processes proteins move between lipid membranes, i.e., in mitochondria, in the endoplasmic reticulum, or near the nucleus envelope, it is desirable to create such an environment in vitro and see the influence of the size of the water lumen. Here we use the FCS to study lysozyme diffusion in hexaethylene glycol monododecyl ether ($C_{12}E_6$) buffered solutions. The choice of the surfactant was dictated by the precise knowledge of its thermodynamic,[32] elastic,[33,34] dynamic, and structural behaviors[35−38] in water solutions.

Materials and Methods

The solutions studied consisted of nonionic surfactant $C_{12}E_6$, phosphate buffer (0.02 M, pH = 7, I = 0.154 M), and lysozyme labeled with 5(6)-carboxytetramethylrhodamine-*N*-hydroxysuccinimide ester (TAMRA) fluorescent dye. The phosphate buffer ionic strength was set to a physiological one (0.154 M) by addition of NaCl. Solutions were prepared by weight and were mixed on a magnetic stirrer with heating to ensure homogeneity of the solution of lyotropic liquid crystal formed. Highly purified by repeated crystallization (three times crystallized) and dialysis lysozyme protein was purchased from Sigma-Aldrich (catalog no. L7651). This small protein can be described as a prolate ellipsoid with short and long axes of 30 and 50 Å, respectively (based on the crystallographic structure). Lysozyme was labeled with the TAMRA fluorescent dye with the absorption and emission in the region of 555 and 580 nm, respectively. The TAMRA fluorescent dye was purchased from Sigma-Aldrich (catalog no. C4759). The nonionic surfactant hexaethylene glycol monododecyl ether ($C_{12}E_6$, catalog no. 52044) of purity better than 98% was purchased from Fluka. The melting temperature given by Fluka Chemical Co. for pure $C_{12}E_6$ was between 27 and 28 °C, and our measurement using differential scanning calorimetry gave 27.11 °C. The molecular weight of the surfactant is 450.66 g/mol. The phase diagram of $C_{12}E_6$ and water is shown in Figure 1.[39] The precise calorimetric study of the diagram has been done recently.[32] The surfactant is miscible with water in the whole range of concentrations up to 38 wt % of $C_{12}E_6$ for temperatures between 0 and 50 °C. The schematic representation of the structures formed in particular phases is shown in Figure 2. Although the phase diagram was established relatively easily, the structure of the isotropic mixture of H_2O and $C_{12}E_6$ has been a matter of some controversy for a long time.[40−42] At very low concentrations and low temperatures (below 20 °C and below 0.1% of surfactant by weight) we expect spherical micelles in the system. At higher concentrations micelles grow in length and eventually form a network[36,38] at

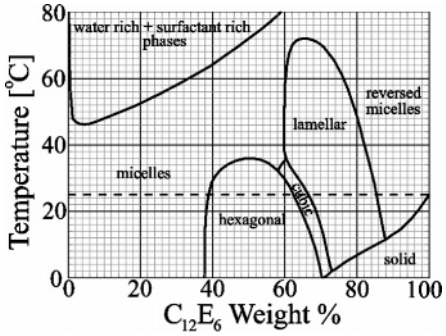

Figure 1. Phase diagram of the nonionic surfactant $C_{12}E_6$/water system. The horizontal dashed line indicates the temperature at which the experiments were carried out.

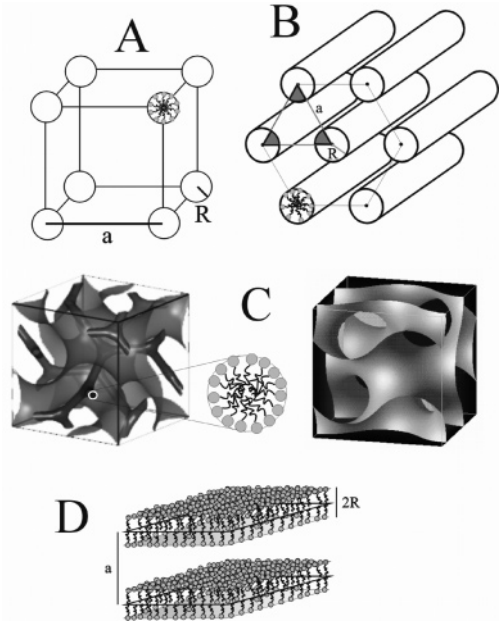

Figure 2. Structures formed in different phases (except for reversed micelles) and the positions of the surfactant molecules: (A) micellar isotropic phase, (B) hexagonal phase, (C) cubic phase, (D) lamellar phase. 2*R* stands for the width of the surfactant structures (micelles, rods, or layers), and *a* is the lattice parameter. On the left picture of the cubic phase one can see two surfactant media represented by rods separated by a surface surrounded with water film. The right picture shows the Schoen gyroid surface (minimal triply periodic surface). When we decorate both of the sides of this surface with water film of the width *L*/2, we obtain the shape of the water film in the cubic phase formed in $C_{12}E_6$/water solution.

concentrations close to the isotropic hexagonal phase transition that occurs at 38 wt % surfactant (Figure 1). We have checked that in the solutions of $C_{12}E_6$ with phosphate buffer (pH 7, I = 0.154 M) the transition temperatures occur in the same region as in the $C_{12}E_6$/water solutions.

From the measurements of the thickness of $C_{12}E_6$ film adsorbed on amorphous silica surfaces from water solutions one can estimate the typical size of the molecules inside a bilayer or micelle. The overall thickness of the bilayer was found to be equal to 50 Å, and the area per headgroup was 40−50 Å^2.[43] The X-ray scattering[35,37] performed on the hexagonal phase indicates that the diameter of the columns in this phase is 44 Å and the size of the unit cell is 58−60 Å. Therefore the average size of the molecule in the bilayer is 25 Å, and in the hexagonal column 22 Å. The cubic phase formed in this system is an example of a bicontinuous structure where two equivalent surfactant media are separated by a water film.[44] The structure of the cubic phase with space group *Ia*3*d* is described by a

Schoen gyroid surface (Figure 2). The value for the cubic lattice parameter is 113−118 Å.[44,45] The estimates for the radius of the micelles at infinite dilution are 32−37 Å.[41,46,47]

Fluorescence Correlation Spectroscopy. In the FCS experiment, the fluorescence intensity emitted from a small volume element of solution, optically defined as the focal volume of the confocal microscope objective, is recorded as a function of time. The recorded fluorescence fluctuates as the fluorescently labeled molecules diffuse in and out of the focal volume or change their photophysical properties. The focal volume is on the order of 1 fL (i.e., 10^{-15} liter), and the concentration of the fluorescent molecules is in the nanomolar range, so it makes the FCS an example of a single-molecule detection technique. Given the average time t a molecule spends in the focal volume and dimensions r of this volume we can derive the self-diffusion coefficient of the molecule ($r^2 \sim Dt$). The fluorescence intensity fluctuations time series can be analyzed by means of the autocorrelation function, which contains the information about the average number of fluorescent molecules in the focal volume, their average resident time in the focal volume, and photophysical properties. The normalized autocorrelation function is given by[49]

$$G(\tau) = \frac{\langle F(t)F(t+\tau)\rangle}{\langle F(t)\rangle^2} - 1 = \frac{\langle \delta F(t)\delta F(t+\tau)\rangle}{\langle F(t)\rangle^2} \quad (1)$$

where $\delta F(t) = F(t) - \langle F\rangle$ is the fluctuation amplitude at a time t.

The laser intensity profile in the region of focal volume is commonly described as a three-dimensional Gaussian

$$I(\mathbf{r}) = I_0 \exp\left(-\frac{2(x^2+y^2)}{{\omega_{xy}}^2} - \frac{2z^2}{{\omega_z}^2}\right) \quad (2)$$

although one should be aware of the possible experimental artifacts arising from the non-Gaussian shape of the focal volume.[50]

The autocorrelation function adopts different analytical forms depending on the assumed physicochemical processes taking place in the studied solution.[51] For the case of three-dimensional isotropic multicomponent diffusion with the triplet state correction this equation takes the form of

$$G(t) = \left(1 + \frac{p}{1-p}\,\mathrm{e}^{-t/\tau}\right)\left(\frac{1}{N}\right)\sum_{i=1}^{n}\frac{A_i}{\left(1+\left(\frac{t}{\tau_{Di}}\right)^{\alpha}\right)\left(1+\frac{1}{\omega^2}\left(\frac{t}{\tau_{Di}}\right)^{\alpha}\right)^{1/2}} \quad (3)$$

where p is the fraction of dye molecules in the triplet state, τ is the triplet lifetime, N is the average number of the molecules in the focal volume, τ_{Di} is the residence time of the molecule in the focal volume, $\omega = \omega_z/\omega_{xy}$ is the structure parameter describing the ratio between longitudinal and transverse size of the focal volume, α is the anomality index ($\alpha = 1$ for normal three-dimensional diffusion and $0 < \alpha < 1$ for anomalous diffusion), A_i is the fraction of the ith component, and n is the number of diffusing species (e.g., a free dye and a protein-bound dye are the two objects ($n = 2$) with different diffusion coefficients).

For normal two-dimensional diffusion, where

$$\langle r^2(t)\rangle = 4Dt \quad (4)$$

the residence time τ_D is related to the diffusion coefficient D by

$$D = \frac{{\omega_{xy}}^2}{4\tau_D} \quad (5)$$

The transverse radius ω_{xy} of the focal volume is taken from the calibration measurement of the residence time τ_{cal} of the fluorescent dye with the known diffusion coefficient D_{cal}

$${\omega_{xy}}^2 = 4D_{cal}\tau_{cal} \quad (6)$$

Finally we can write the simple expression relating the diffusion coefficient D of the studied molecule to the diffusion coefficient of the fluorescent dye D_{cal} used for calibration and their residence times

$$D = D_{cal}\frac{\tau_{cal}}{\tau_D} \quad (7)$$

For anomalous two-dimensional diffusion where

$$\langle r^2(t)\rangle = 4\Gamma t^{\alpha} \quad (8)$$

we have the transport coefficient Γ with the dimensions of area per fractional time ($\mu m^2/s^{\alpha}$) given by[17,20,23]

$$\Gamma = \frac{{\omega_{xy}}^2}{4{\tau_D}^{\alpha}} \quad (9)$$

By the analogy to the equation (eq 4) for normal diffusion we can write

$$\langle r^2(t)\rangle = 4\Gamma t^{\alpha-1}t = 4D(t)t \quad (10)$$

and define

$$D(t) = \Gamma t^{\alpha-1} \quad (11)$$

as the time-dependent diffusion coefficient. As the estimate of the anomalous diffusion coefficient we will give the value of the time-dependent diffusion coefficient at a time τ_D (with dimensions of $(\text{length})^2(\text{time})^{-1}$), i.e.,

$$D(\tau_D) = \Gamma {\tau_D}^{\alpha-1} \quad (12)$$

FCS Setup. One-color FCS measurements (autocorrelation) were carried out at 25 °C on a commercial system (ConfoCor II, Carl Zeiss, Jena, Germany) using a 543 nm He−Ne laser for illumination. The details of the experimental setup can be found elsewhere.[52] The used objective was a C-Apochromat 40×/1.2 (N. A. 1.2). The pinhole diameter was set to 78 μm (1 Airy unit for a 543 nm laser) for all shown measurements. An Avalanche photodiode was used as a detector. The laser intensities used were about 40 μW (power density at the focal point ~30 kW/cm^2). The accessible time range for the measurements of the autocorrelation function was from 1 μs to 10 s.

To exclude the possibility of the non-Gaussian shape of the confocal volume, free diffusion of rhodamine 6G in water was measured prior to each experiment and obtained data fitted well with the single-component autocorrelation function for normal diffusion ($\alpha = 1$, $n = 1$, eq 3). The value of the fitted structure parameter ω for rhodamine 6G amounted to about 5. The diffusion coefficient for rhodamine 6G at 20 °C is 2.8×10^{-6} cm^2/s,[53] which corresponds to a diffusive time τ of 31 μs in

our FCS setup. It gives the following dimensions of the focal volume: $\omega_{xy} = 0.186(3)$ μm, $\omega_z = 0.932(15)$ μm. At least 20 correlation functions accumulated for 30 s were recorded for each solution, and their average was analyzed with Origin in the nonlinear least-squares fitting module and by the MEMFCS program[54] based on the maximum entropy method. The standard deviation of the values of the autocorrelation function was calculated as the standard deviation of the average and used for the calculation of the χ^2 test. The basic idea of MEMFCS is as follows: It assumes a wide range of the expected times τ_D and chooses the widest distribution of times consistent with the data and providing a low χ^2 value. It uses eq 3 with the fixed values of τ_D spanned on the logarithmic scale ($n = 100$ with each sum element corresponding to one τ_D) and fits the amplitudes A_i to achieve agreement for all data. The values of N, τ, and p are not subject to optimization and have to be given constant values. The quality of the fit is estimated with χ^2 with the uncertainties calculated as the root-mean-square deviation of the points of the average autocorrelation function. It is often possible that a good fit criterion is satisfied for many different distributions of A_i, so the final solution is chosen according to the maximum entropy principle. The entropy is defined as $S = \sum_{i=1}^{n} p_i \ln p_i$, where $p_i = A_i/\sum A_i$. The distribution of A_i that minimizes χ^2 and maximizes S is chosen. The distribution is improved in successive iterations of optimization that use the search directions constructed using the derivatives of S and χ^2. As was mentioned by ref 17, the analysis of data should be done using both models, i.e., normal and anomalous diffusion. Then the quality of fits and physical content of the obtained parameters of both models should be compared. On the basis of this comparison and the knowledge of the physical parameters characterizing the studied system the best model should be selected. Below we follow this procedure.

Results

Fits Assuming Normal Diffusion. First we fitted the obtained ACFs using the normal diffusion model. In the concentration range of the surfactant from 0.05% to 1%, the single-component normal diffusion model fitted very well to the experimental data, and no influence of the surfactant on the diffusion coefficient of the lysozyme was observed. From the concentration of about 4% a second slower process, with a relative amplitude up to 10%, started to appear, and a two-component normal diffusion model was necessary to fit the experimental data satisfactory (Figure 3). The amplitudes of the two modes are shown in Figure 4. The diffusion coefficient started to decrease from the concentration of about 3% (Figure 5). After the concentration reached the end of the liquid phase (~37%) the value of the diffusion coefficient of the fast process decreased to 0.06×10^{-6} cm^2/s. From the analysis of the size of the water channels (Appendix) in the $C_{12}E_6$/water system we can see that the size of the water channel decreases with increasing surfactant concentrations and approaches the size of the lysozyme molecule for the solution with 37% of surfactant. It means that the lysozyme molecule starts to squeeze through the water channels and its diffusion remains on the slowest possible level, and no slow process can be attributed for the lysozyme monomer. The observed long residence time and thus very small diffusion coefficient (shown in Figure 3) with a relative amplitude up to 10% (Figure 4) could correspond to the lysozyme entrapped in the dense local structures formed by surfactant but should not decrease further than the limit of 0.06×10^{-6} cm^2/s, as the latter corresponds to the slowest diffusional movement attributed to the lysozyme monomer. As the small diffusion coefficient corresponding to the long residence time approaches the limit

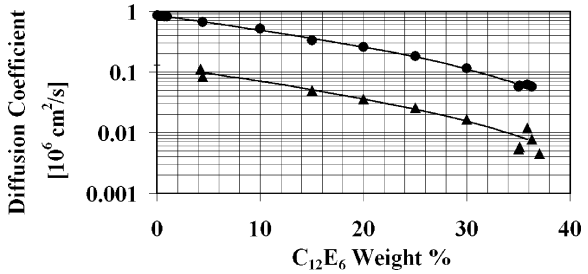

Figure 3. Fit of the normal diffusion model resulting in two-component diffusion. The faster process with a relative amplitude of at least 90% corresponds to the lysozyme monomer diffusion (circles). The slower process with a relative amplitude up to 10% corresponds to very slow diffusion (triangles) due to the protein−micelle complexes. The long diffusion time, corresponding to the lysozyme−micelle complexes, was not detected for all concentrations above the CMC of the surfactant but only concentrations larger than 4%. It suggests that the interaction of proteins and micelles is rather weak and hard to observe in diluted samples. Also in the highly concentrated solution (37%), where the distance between the micelles is comparable to the protein size, the amplitude (Figure 4) in the signal for the protein−micelle complex was only 10% of the total signal, leaving 90% for the free proteins.

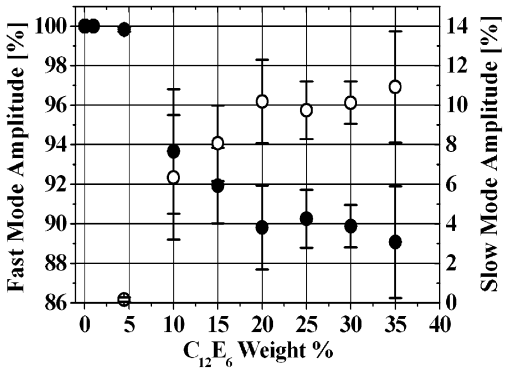

Figure 4. Amplitudes of the slow diffusion and fast diffusion (shown in Figure 3). The amplitude of the fast mode decreases with surfactant concentration while the slow diffusion amplitude increases with the concentration. This behavior is consistent with the hypothesis of the formation of protein−micelles complexe. The fact that we could not observe the slow diffusion process for diluted samples means that the protein−micelle interactions (association) are rather weak.

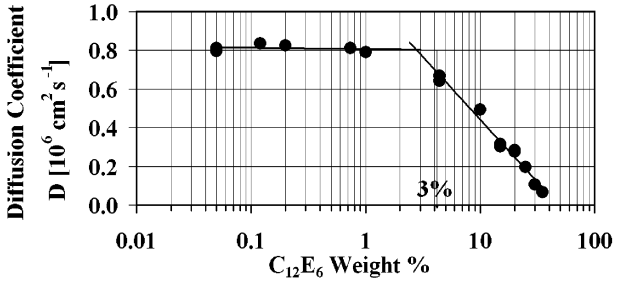

Figure 5. Lysozyme monomer diffusion. For a concentration of about 3% the diffusion coefficient starts to decrease. The solid lines through the data are guides to the eye only.

of 0.005×10^{-6} cm^2/s (for 37% of $C_{12}E_6$), we do not ascribe this diffusion to the protein but rather to the micelle−protein complex. Such complexes should appear already for concentrations higher than the critical micelle concentration (CMC) for $C_{12}E_6$. The CMC for the $C_{12}E_6$ nonionic surfactant[40] is 0.002% at 25 °C, so the lysozyme−micelle complexes should be present for all concentrations in the micellar phase studied in the present work. However for concentrations up to 4% no long residence time was observed in the studied samples. This fact is mainly due to the very weak interactions of between the micelle and

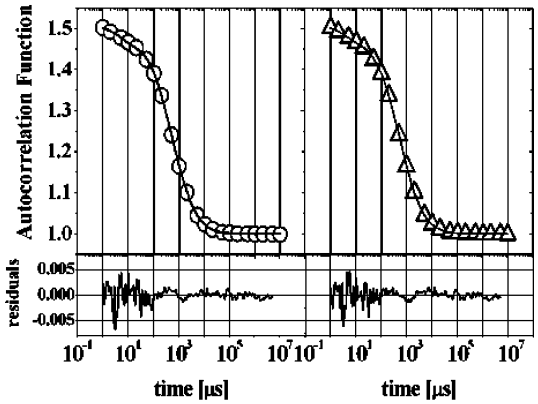

Figure 6. Autocorrelation function collected in the solution of $C_{12}E_6$ (25 wt %) fitted with normal diffusion (left figure) and anomalous diffusion (right figure). Both curves fit well to the experimental data giving the following parameters: two-component normal diffusion ($\tau_1 = 454$ μs with a fraction of 90%, $\tau_2 = 2307$ μs with a fraction of 10%); one-component anomalous diffusion ($\tau_1 = 551$ μs, anomality index $\alpha = 0.925$) (τ_1 and τ_2 are the resident times in the focal volume). Both fits are very good, and none of them can be ruled out solely on the basis of fits.

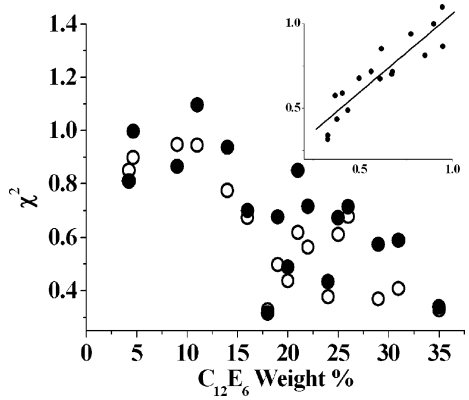

Figure 7. χ^2 values obtained for the fits with two models of isotropic three-dimensional diffusion (empty circles, two-component normal diffusion; filled circles, one-component anomalous diffusion). Both fits gave very similar values of the χ^2 test, but in the anomalous diffusion model we fit six parameters (N, p, τ, τ_{D1}, α,and ω) instead of seven parameters (N, p, τ, τ_{D1}, τ_{D2}, A_1, and ω) in the case of two-component normal diffusion. On the inset graph the values of χ^2 for both models are plotted (with anomalous diffusion (ordinate) versus normal diffusion (abscissa)). The resulting straight line shows that the χ^2 test gave similar values for both models.

the protein. In fact the amplitude of the slow diffusion mode grows very slowly with the concentration of $C_{12}E_6$, indicating that protein does not attach easily to the nonionic surfactant. That is why for very small concentrations of micelles the slow process is hard to observe.

Fits Assuming Anomalous Diffusion. Because the anomalous diffusion was invoked in the interpretation of protein movement in concentrated solutions we have also analyzed the data using the anomalous diffusion model. The quality of the single-component anomalous diffusion fit was as good as the two-component fit using the normal diffusion model (Figures 6 and 7).

In the micellar phase the anomality index was gradually decreasing with increasing surfactant concentration (Figure 8). The residence time obtained when fitting the data with anomalous diffusion was very similar to the shorter time of the two obtained for normal diffusion. This means that the time-dependent diffusion coefficient $D(\tau)$ is the same as the shortest diffusion coefficient (eq 12, compare Figure 9 to Figure 3). The

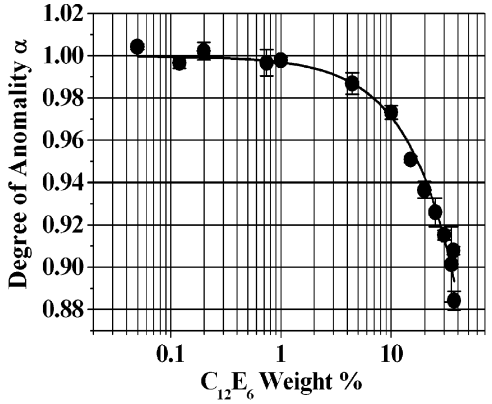

Figure 8. Dependence of the anomality index α on the concentration of $C_{12}E_6$. The anomality index decreases as the micelles grow in length (surfactant concentration increases). For small concentrations up to about 3%, we observe normal diffusion ($\alpha \approx 1$).

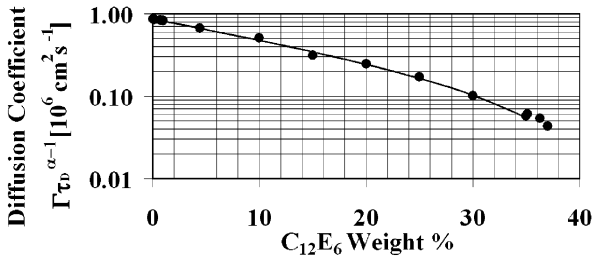

Figure 9. Diffusion coefficients obtained by fitting the data with the anomalous diffusion model. The diffusion coefficient in anomalous diffusion depends on time, and here we simply show its value for the resident time, i.e., for the time a protein stays in the focal volume. (see also Figure 3).

two-component normal diffusion model has a very clear physical interpretation while the anomalous diffusion does not. Moreover the anomality index does not tell us much about the physical process that led to the occurrence of anomality. Usually anomalous diffusion is attributed to the process in which a diffusing object falls into the trap with an algebraic distribution of trapping times.

In summary, a two-component normal diffusion model is much easier to interpret physically than the anomalous diffusion model.

Conclusions

We have observed, using FCS, that lysozyme protein moves by diffusion in $C_{12}E_6$ nonionic surfactant buffered solutions. We have presented two different models (two-component normal diffusion and anomalous diffusion) and fit them to experimental results. One of them assumes that the protein moves by diffusion with two dramatically different (1 order of magnitude) diffusion coefficients. The amplitude of the slow diffusion coefficient grows with $C_{12}E_6$ concentration, and both diffusion coefficients decreased by an order of magnitude from pure water to the concentrated surfactant solution (37% of $C_{12}E_6$). The second model assumed the anomalous diffusion for this movement. Both models gave fits of the same quality with a smaller number of fit parameters for anomalous diffusion, but purely on this basis we could not distinguish which of the models is better. On the physical basis the two-component normal diffusion model had a perfect explanation. The proteins interact with micelles forming protein−micelle complexes. One of the diffusion coefficients (large) is due to free protein diffusion, while the slow one is due to the protein−micelle complex. The weak interaction precluded the observation of the slow process at high

dilution (less than 4% of $C_{12}E_6$). The amplitude of the slow mode grows slightly (weak association of proteins) with surfactant concentration reaching 10% of the signal for 37% surfactant solution. It should be noted that for 37% surfactant solution the distance between the micelles (Appendix) is comparable to the size of the protein; thus the latter has to squeeze between the micelles during the diffusive motion.

Acknowledgment. We thank Professor Periasamy for providing the MEMFCS program for the analysis of the FCS data. This work has been supported as a scientific project during 2004−2007 (grant 3T09A09727) and 2006−2008 from the science budget of the Polish Ministry of Education and Science.

Appendix

Average Size of the Water Channels in the Structures Formed by the Nonionic Surfactant $C_{12}E_6$−Phosphate Buffer System. To make more detailed insight into diffusion processes taking place in our system we estimated the average size of the water channels in the formed structures (Figure 10). We related the volume fraction of the surfactant to the parameters describing the arrangement of the water and surfactant molecules in each of the phases. The derived relations allowed for the calculation of the size of the water channels. Below we compute the size of the water channels, *S*, from the knowledge of the structure of the system i.e., volume fraction of surfactant and the structure formed by the surfactant.

The relation between the volume fraction for the spherical micelles in the simple cubic geometry and the size of the unit cell *a* (see Figure 2) is given by

$$a = \left(\frac{4\pi}{3\phi}\right)^{1/3} R \tag{13}$$

where *R* is the micelle radius. The size of the water channel *S*, given as the cubic unit cell wall diagonal, decreased by the diameter of the micelle, can be expressed in terms of volume fraction ϕ of surfactant and radius *R* (34 Å)

$$S = a\sqrt{2} - 2R = \left(\left(\frac{4\pi}{3\phi}\right)^{1/3}\sqrt{2} - 2\right)R \tag{14}$$

For the hexagonal phase the volume fraction can be expressed as a function of the cylinder radius, *R*, and the size of the hexagonal unit cell *a*

$$\phi = \frac{\frac{\pi R^2}{2}}{\frac{a^2\sqrt{3}}{4}} = \frac{2\pi R^2}{a^2\sqrt{3}} \tag{15}$$

hence

$$a = \sqrt{\frac{2\pi}{\phi\sqrt{3}}}R \tag{16}$$

An estimate for *S* is given as the diameter of the sphere inscribed between the cylinders

$$S = 2\left[\frac{a\sqrt{3}}{3} - R\right] = 2R\left[\sqrt{\frac{2\pi}{\phi 3\sqrt{3}}} - 1\right] \tag{17}$$

where *R* is the radius of the cylinder (22 Å)

For the lamellar phase we can write

$$\phi = \frac{2R}{a} \tag{18}$$

hence

$$a = \frac{2R}{\phi} \tag{19}$$

and the diameter *S* of the inscribed sphere is given by

$$S = 2R\left(\frac{1}{\phi} - 1\right) \tag{20}$$

where *R* is the half of the width of the lamellar plane ($R = 25$ Å)

The volume inside a cubic gyroid phase occupied by the water film, when the triply periodic minimal surface in the unit cell is symmetrically decorated with the water layer of the length $L/2$, is given by

$$V = s_0 L + \frac{\pi}{6}\chi L^3 \tag{21}$$

thus for the cubic phase volume fraction of water (ϕ is the volume fraction of the surfactant; hence $(1 - \phi)$ is the volume fraction of water) is given by

$$1 - \phi = \frac{V}{a^3} = s^*_0 L^* + \frac{\pi}{6}\chi L^{*3} \tag{22}$$

where $s^*_0 = s_0/a^2$ is the dimensionless surface area of the triply periodic minimal surface (TPMS) per unit cell with the cell parameter *a*, $L^* = L/a$ is the dimensionless layer width, and χ is the Euler characteristics per unit cell. For the Schoen gyroid surface the Euler characteristics per unit cell $\chi = -8$, and the dimensionless surface area of the triply periodic surface per unit cell $s^*_0 = 3.0966$.[55] The size of the water channel was obtained by solving the third-order equation (eq 22) for L^*, and the width of the water channel was $L = L^*a$, where *a* is the cubic lattice parameter (118 Å). Figure 10 shows the size of the water channels as a function of the surfactant concentration.

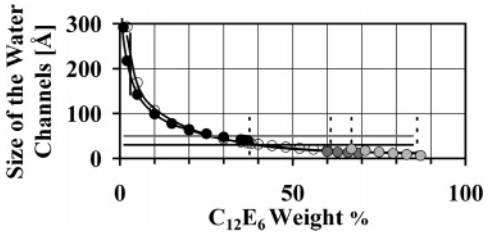

Figure 10. Average size of the water channels in the structures formed by $C_{12}E_6$/water solutions. The values presented in the figure were obtained from the following equations: micelles, black circles (eq 14); elongated micelles and hexagonal phase, white circles (eq 17); lamellar phase, light gray circles (eq 20); cubic phase, dark gray circles (eq 22). The full black lines are shown as a guide for the eye. At a temperature of 25 °C one observes four phase transitions as a function of concentration. Phases occur in the following order (from left to right): micelles, hexagonal, cubic, lamellar, and reversed micelles. The concentrations where phase transitions occur are indicated with vertical dashed lines. The long (50 Å) and short (30 Å) axes of the lysozyme molecule are indicated with gray and black horizontal lines. The concentration (3%) where the diffusion coefficient of the lysozyme starts to decrease (Figure 8) is indicated with a full black vertical line. For this concentration the size of the water channel amounts to about 4−6 diameters of the lysozyme molecule. For 37% surfactant the size of the water channels is comparable to the protein size.

Densities of the studied solutions are very close to 1 g/cm^3,[56] so there is practically no difference between the volume fraction and the weight fraction, the latter being used to express the concentration in our experiment.

References and Notes

(1) Record, T. M., Jr.; Courtenay, E. S.; Cayley, S.; Guttman, H. J. *Trends Biochem Sci.* **1998**, *23*, 190.
(2) Rivas, G.; Ferrone, F.; Herzfeld, J. *EMBO Rep.* **2003**, *5*, 23.
(3) Weiss, M.; Elsner, M.; Kartberg, F.; Nilsson, T. *Biophys. J.* **2004**, *87*, 3518.
(4) Elowitz, M. B.; Surette, M. G.; Wolf, P. E.; Stock, J. B.; Leibler, S. *J. Bacteriol.* **1999**, *181*, 197.
(5) Swaminathan, R.; Hoang, C. P.; Verkman, A. S. *Biophys. J.* **1997**, *72*, 1900.
(6) Dayel, M. J.; Horn, E. F. Y.; Verkman, A. S. *Biophys. J.* **1999**, *76*, 2843.
(7) Phair, R. D.; Mistell, T. *Nature* **2000**, *404*, 604.
(8) Partikian, A.; Olveczky, B.; Swaminathan, R.; Li, Y.; Verkman, A. S. *J. Cell Biol.* **1998**, *140*, 821.
(9) Luby-Phelps, K.; Castle, P. E.; Taylor, D. J.; Lanni, F. *Proc. Natl. Acad. Sci. U.S.A.* **1987**, *84*, 4910.
(10) Kao, H. P.; Abney, J. R.; Verkman, A. S. *J. Cell Biol.* **1993**, *120*, 175.
(11) Verkman, A. S. *Trends Biochem. Sci.* **2002**, *27*, 27.
(12) Yokoe, H.; Mayer, T. *Nat. Biotechnol.* **1996**, *14*, 1252.
(13) Gambin, Y.; Massiera, G.; Ramos, L.; Ligoure, C.; Urbach, W. *Phys. Rev. Lett.* **2005**, *94*, 110602.
(14) Feder, T. J.; Brust-Mascher, I.; Slattery, J. P.; Baird, B.; Webb, W. W. *Biophys. J.* **1996**, *70*, 2767.
(15) Periasamy, N.; Verkman, A. S. *Biophys. J.* **1998**, *75*, 557.
(16) Brown, E. B.; Wu, E. S.; Zipfel, W.; Webb, W. W. *Biophys. J.* **1999**, *77*, 2837.
(17) Saxton, M. J. *Biophys. J.* **2001**, *81*, 2226.
(18) Magde, D.; Elson, E. L.; Webb, W. W. *Phys. Rev. Lett.* **1972**, *29*, 705.
(19) Eigen, M.; Rigler, R. *Proc. Natl. Acad. Sci. U.S.A.* **1994**, *94*, 11753.
(20) Schwille, P.; Korlach, J.; Webb, W. W. *Cytometry* **1999**, *36*, 176.
(21) Banks, D. S.; Fradin, C. *Biophys. J.* **2005**, *89*, 2960.
(22) Knackstedt, M. A.; Ninham, B. N.; Monduzzi, M. *Phys. Rev. Lett.* **1995**, *75*, 653.
(23) Fatin-Rouge, N.; Starchev, K.; Buffle, J. *Biophys. J.* **2004**, *86*, 2710.
(24) Weiss, M.; Hashimoto, H.; Nilsson, T. *Biophys. J.* **2003**, *84*, 4043.
(25) Arnold, A.; Paris, M.; Auger, M. *Biophys. J.* **2004**, *87*, 2456.
(26) Levi, V.; Ruan, Q.; Gratton, E. *Biophys. J.* **2005**, *88*, 2919.
(27) Saxton, M. J. *Biophys. J.* **1994**, *66*, 394.
(28) Bouchaud, J. P.; Georges, A. *Phys. Rep.* **1990**, *195*, 127.
(29) Hołyst, R.; Błażejczyk, M.; Burdzy, K.; Góralski, G.; Bocquet, L. *Physica A* **2000**, *277*, 71.
(30) Burdzy, K.; Hołyst, R. *Phys. Rev. E* **2001**, *64*, 011914.
(31) von Hippel, P. H.; Berg, O. G. *J. Biol. Chem.* **1989**, *264*, 675.
(32) Nishizawa, M.; Saito, K.; Sorai, M. *J. Phys. Chem. B* **2001**, *105*, 2987.
(33) Oswald, P.; Allain, M. *J. Phys.* **1985**, *46*, 831.
(34) Sallen, L.; Oswald, P.; Geminard, J. C.; Malthete, J. *J. Phys. II* **1995**, *5*, 937.
(35) Sallen, L.; Sotta, P.; Oswald, P. *J. Phys. Chem. B* **1997**, *101*, 4875.
(36) Constantin, D.; Oswald, P. *Phys. Rev. Lett.* **2000**, *85*, 4297.
(37) Constantin, D.; Oswald, P.; Imperor-Clerc, M.; Davidson, P.; Sotta, P. *J. Phys. Chem. B* **2001**, *105*, 668.
(38) Constantin, D.; Freyssingeas, E.; Palierne, J. F.; Oswald, P. *Langmuir* **2003**, *19*, 2554.
(39) Mitchel, D. J.; Tiddy, G. J. T.; Waring, L.; Bostock, T.; McDonald, M. P. *J. Chem. Soc., Faraday Trans. 1* **1983**, *79*, 975.
(40) Strey, R. *Ber. Bunsen−Ges. Phys. Chem.* **1996**, *100*, 182.
(41) Brown, W.; Johnsen, R.; Stilbs, P.; Lindman, B. *J. Phys. Chem. B* **1983**, *87*, 4548−4553.
(42) Lindman, B.; Wennestrom, H. Nonionic micelles grow with increasing temperature. *J. Phys. Chem.* **1991**, *95*, 6053.
(43) McDermott, D. C.; Lu, J. R.; Lee, E. M.; Thomas, R. K. *Langmuir* **1992**, *8*, 1204.
(44) Clerc, M.; Levelut, A. M.; Sadoc, J. F. *J. Phys. II* **1991**, *1*, 1263.
(45) Imperor-Clerc, M.; Levelut, A. M. *Eur. Phys. J. E* **2001**, *4*, 209.
(46) Zulauf, M.; Weckstrom, K.; Heyter, J. B.; Degiorgio, V.; Corti, M. *J. Phys. Chem.* **1985**, *89*, 3411
(47) Kato, T.; Seimiya, T. *J. Phys. Chem.* **1986**, *90*, 3159.
(48) Yethiraj, A.; Capitani, D.; Burlinson, N. E.; Burnell, E. E. *Langmuir* **2005**, *21*, 3311.
(49) Elson, E. L.; Magde, D. Fluorescence *Biopolymers* **1974**, *13*, 1.
(50) Hess, S.; Webb, W. W. *Biophys. J.* **2002**, *83*, 2300.
(51) Krichevsky, O.; Bonnet, G. *Rep. Prog. Phys.* **2002**, *65*, 251.
(52) Jankowski, T.; Janka, R. *Fluorescence Correlation Spectroscopy, Theory and Applications*; Rigler, R., Elson, E. S., Eds.; Springer Series in Chemical Physics 65; Springer-Verlag: Heidelberg, 2001; p 331.
(53) Magde, D.; Elson, E. L.; Webb, W. W. *Biopolymers* **1974**, *13*, 29.
(54) Sengaputa, P.; Garai, K.; Balaji, J.; Periasamy, N.; Maiti, S. *Biophys. J.* **2003**, *84*, 1977.
(55) Garstecki, P.; Hołyst, R. *Langmuir* **2002**, *18*, 2519.
(56) Maccarini, M.; Briganti, G. *J. Phys. Chem. A* **2000**, *104*, 11451.